Horizontal Saddle Supported Storage Vessels: A Parametric Study of Plastic Collapse Loads

A S Tooth, G C M Chan, J Spence and D H Nash
Department of Mechanical Engineering, University of Strathclyde,
75 Montrose Street, Glasgow, G1 1XJ, UK

ABSTRACT

Previous work by the present authors compared various theoretical methods with simple experiments for the plastic collapse load on end supported vessels loaded centrally by rigid saddles. It was found that the best agreement was obtained by using an elastic-plastic finite element analysis approach. In the present paper the elastic-plastic method has been used to examine the effect of various geometric parameters on the collapse load. A symmetrical model which replicated the geometric features of the experiments can be used to give an indication of the effect of specific isolated geometric variables but for others and for the purposes of undertaking a full parametric survey the model was modified to reflect an actual twin saddle supported vessel.

It was found that when the saddle width and/or the saddle embracing angle increased, the collapse load increased; also when the overall length of the vessel increased, the collapse load decreased. An important parameter dictating the plastic collapse load for actual vessel geometries is the distance from the vessel head to the saddle centre. With the modified model a theoretical parametric survey was conducted on a range of vessel geometries with both welded and loose saddle configurations. The collapse loads from the survey are presented as a series of graphs and also in the form of simple equations for use in design.

NOTATION

A Longitudinal distance to the saddle support centre line from the end of the cylindrical shell (mm)
b_1 Width of saddle (mm)
L Barrel length of the vessel (mm)

L_S Longitudinal distance between saddle supports (mm)
R Mean radius of vessel (mm)
t Shell thickness of vessel (mm)
σ_y Tensile yield strength of shell material (N/mm^2)
2α Saddle embracing angle (degrees or radians)
P Parametric collapse load by elastic-plastic analysis (kN)

1 INTRODUCTION

Horizontal vessels are widely used as storage vessels for liquids or gaseous products. Such vessels are commonly supported above ground by twin saddle supports, Fig 1(a). The saddle supports are normally welded on to the vessels or loosely placed. Present design rules (1) can greatly underestimate the carrying capacity of the vessel as the stresses are highly localised in the region of the saddle horns whilst the rest of the vessel is only moderately stressed. An alternative approach is to base the design of the vessel on the maximum carrying capacity, i.e., the collapse load. The advantage of this approach is that it provides the designer with a method of finding an allowable load directly by dividing the collapse load by a factor, usually 1.5. This procedure avoids the necessity of categorising the maximum stresses. This method is, of course, only useful if fatigue is not included in the design requirements.

The experimental plastic collapse loads of end supported vessels loaded centrally through a "rigid" saddle, Fig. 1(b), which is either welded or placed loosely on the vessel have been examined previously by the authors (2). This arrangement is termed "the end supported inverted case". It was found that there are two main modes of failure, a plastic collapse mode and a more sudden elastic buckling mode. Plastic collapse occurred when the vessel's radius to shell thickness was relatively small (R/t<214) and is characterised by the gradual formation of plastic hinges which cause the eventual collapse of the vessel.

A number of theoretical approaches to the plastic collapse load for this inverted arrangement for both welded and loose saddles have been reported (3). The methods examined include various limit analysis and finite element approaches. The paper concluded that the best estimate of the collapse load was obtained from an elastic-plastic finite element method. The good comparisons with experiments provided the justification for the application of the method to a wider range of vessel parameters.

The main purpose of this present paper is to report the results of a parametric survey on saddle supported vessels for the plastic collapse load using the elastic-plastic method. Both welded and loose saddles are covered and the effects of saddle embracing angle, saddle width, vessel length and head to saddle centre distance have been investigated.

2 FINITE ELEMENT MODEL - end supported inverted case

The model used in Ref. (3) is first briefly described and then used to explore the effects of some of the variables. The finite element model for all of the elastic-plastic analysis employed 4-noded shell elements to represent the shell and 8-noded brick elements for the saddle. Since the saddle widths were reasonably narrow, one element through thickness was sufficient. The

finite element package used throughout was ANSYS (4). The F.E. model was developed to replicate the experimental set-up of a cylindrical vessel loaded centrally by a saddle at its mid-span, see Fig. 1(b). Essentially this assumes that collapse is a local phenomenon and a model length of approximately 4*R* is sufficient to avoid interaction effects from the ends of the model as suggested originally by Zick (5). This will be discussed later. Symmetry boundary conditions were applied to the longitudinal and transverse sections of the geometry to produce a quarter model. Convergence tests (6) were conducted by varying the mesh density and the element numbers to arrive at a suitably efficient model with 254 elements, Fig.2. The open ends of the model were constrained in the circumferential direction but were free to deform in the radial direction or rotate in their plane. This is an approximation to the experimental boundary conditions (1) where there a degree of radial restraint imposed by thin rings inserted into the open ends of the test cylinder. It is assumed that the load on the saddle is equivalent to half the total load (vessel and contents as appropriate). The vessel was loaded incrementally via pressure acting on the base of the saddle, simulating the applied load. A large deflection analysis was performed and an elastic perfectly plastic stress-strain relationship was assumed. The twice elastic slope method was used as a basis of obtaining the collapse load. This was obtained from a graph plotting the applied total load on the saddle and the vertical displacement of a node on top (i.e. the base) of the saddle.

For the purpose of investigating the effect of various geometric parameters some exploratory calculations were conducted with this end supported inverted model.

2.1 Variation with overall length

To study the variation of the collapse load with the vessel's length and the various saddle parameters, only a welded saddle was considered. For modelling purposes the saddle is "welded" to the vessel by merging the nodes on the boundary of the vessel/saddle interface. The nodes in the interface were not merged together.

The basic dimensions of the model used in this investigation had a vessel radius *R* of 130mm, a shell thickness *t* of 1.57mm and a yield stress σ_y of 222.2 N/mm^2. The vessel was loaded centrally with a rigid saddle with an embracing angle $2\alpha=120^\circ$ and a saddle width b_1 of 10mm. The dimensions reflect an actual end supported experimental vessel which failed by plastic collapse and reported in (2). Twenty-four different cases were explored with the total length varying from *R* to 54*R*. The collapse load results obtained are given in Fig. 3 (with a trendline through the points).

Figure 3 shows that the vessel length has a significant effect on the collapse load. It should be noted that the previous studies based on a length of approximately *4R*, while useful for comparisons between theory and experiment, might need to be treated with care when considering actual vessels.

Two almost linear portions are evident in Fig. 3. The steep slope indicates the effect of the end boundary condition restraint stiffening the vessel; the lower slope portion is considered to be due to the “beam” effect of a long vessel.

2.2 Variation with saddle embracing angle and saddle width

Using the same welded saddle model as in the previous section, the influence of the saddle width b_1 and the saddle embracing angle 2α on the collapse load of the end supported vessel was examined. The following parameters were used, R=130mm, t=1.57mm, σ_y=222.2 N/mm^2, with a length of $4R$ as before. In order to observe the variation of the saddle embracing angle, the width of the saddle was kept constant at 10mm and the saddle embracing angle increased from 40˚ to 160˚. The collapse results are shown in Figure 4 again with a trendline shown. The results show a higher collapse load for a larger saddle embracing angle. This is expected as a larger saddle angle would have a higher contact area and consequently a longer plastic hinge would form as the vessel collapses. More importantly, the graph shows that the increase in collapse load is significant. If the saddle angle is increased from 120˚ to 150˚, the collapse load increases from 38.7 kN to 56.45 kN, an increase of 46%. The variation is also slightly non-linear.

The variation of the collapse load with the saddle width was examined by maintaining the saddle angle at 120˚ and varying the total saddle width b_1 from 10mm to 50mm. As the saddle widths were relatively large, in this case the F.E. model was altered to have three brick elements through the thickness of the saddle. The results are given in Table 1. An increase of 5 times the saddle width (from 10mm to 50mm) results in an increase in collapse load of only 12%.

3 FINITE ELEMENT MODEL - "actual" vessel case

The F.E. models used so far have represented the end-supported inverted case as it relates to the previous experiments reported in (2). It is now proposed to apply the elastic-plastic analysis to a "actual" twin saddle supported vessel for both welded and loose saddle configurations. The vessel has two planes of symmetry about its centre which together divide the vessel into a convenient quarter model as shown in Fig. 5. The F.E. model of this quarter vessel requires different boundary conditions at each extremity. The "head" end was constrained in the circumferential direction (as before). At the "centre" of the vessel, symmetry boundary conditions were applied. The other details of the model in terms of the element types, the loading procedure, material assumptions and definition of collapse load were similar to those used for the end supported inverted case.

In order to represent the welded case, nodes at the vessel/saddle boundary were fully connected. However in the loose saddle case, contact elements were used for all nodes at the interface. These were point-to-point elements and represent two surfaces which may maintain or break physical contact and may slide relative to each other. This contact element is only capable of supporting compression in the radial direction and shear in the circumferential direction; because of a lack of constraint at the vessel/saddle interface, the nodes at the centre line of the saddle were coupled together. This restrains the saddle from moving longitudinally along the vessel. Convergence tests were performed and a final convergent model with 480 elements was selected.

3.1 Comparisons with end supported vessels

As a first step, the actual vessel model is compared with the earlier end supported inverted model. Four different "actual" F.E. models were analysed initially with welded and loose saddles. These models assumed that the vessel is supported at the quarter points along the length of the vessel (i.e. the saddle is positioned centrally on the quarter model and the model

extends from the centre line of the vessel to the junction with the head). The parameters for these models were selected from experimental tests on end supported vessels (2) on the basis that they collapsed in a plastic manner. The geometry of the vessels and the comparisons of the results with the end supported and "actual" cases are tabulated in Table 2. Experimental results from the end supported inverted experiments are included in the table for completeness although they should not be compared directly with the F.E. results from the "actual" model. The table shows that for the welded saddles, the collapse load results for the "actual" F.E. model was about two thirds those of the end supported inverted case F.E. model. However, the collapse load for the loose saddle was similar for both end supported inverted cases and "actual" cases.

Whilst this is not unexpected, an explanation for this difference can be found from a consideration of the development of the plastic zones with increase in load. In the case of a welded model the stiffening effect of the welded saddle allows plastic zones to spread almost throughout the model especially towards the centre. In the case of the loose saddle the development of plastic behaviour and the collapse itself is a rather more local phenomenon. These results confirm that the "actual" vessel model is necessary for the parametric study.

3.2 Tests on different saddle position

In Section 3.1 the saddles were positioned at the quarter points on the vessel which is common practice. However on occasions, the position of the saddle may be moved nearer to the "head" end of the vessel or towards the vessel centre. To investigate the effect of this change, various models of a "real" vessel (based on a vessel with R=130mm, t=1.57mm, σ_y=222.2 N/mm^2, 2α=120˚ and b_1=10mm) with a welded saddle were analysed with different vessel lengths such that the position of the saddle was moved from the quarter point. Similar calculations were carried out for loose saddles (R=130mm, t=1.55mm, σ_y=275 N/mm^2, 2α=120˚ and b_1=10mm). The resulting collapse loads are tabulated in Table 3. The lengths used in the F.E. models such as the distance from "head" to saddle, A, and the distance between saddles (L_S) are expressed in terms of factors of the vessel radius, R.

Examination of the collapse results of the welded saddle show that when the distance to the "head", A, is held constant (at $2R$) and the semi-centre span, $L_S/2$, increased from R *to* $4R$, the collapse load varies from 23.17 kN to 25 kN. When the span is held constant (at $2R$) and the distance from the saddle to the head increased from R to $4R$, the collapse load reduces from 32.17 kN to 15.3 kN. It is evident that the distance of the saddle from the "head" is an important factor when collapse loading is considered.

The loose saddle cases show a similar trend. When the distance to the "head", A, is held constant and the centre span, $L_S/2$, increased from R to $4R$, the collapse loads vary from 20.81 kN to 22.52 kN. When the centre semi-span, $L_S/2$, is held constant (at $2R$) and the distance to the head, A, is increased from R to $4R$, the collapse load reduces from 23.1 kN to 18.4 kN. The drop in collapse load when A is varied is not as large in the loose saddle case as in the case of the welded saddle. This could again be attributed to the localised nature of collapse for loose saddles. However, this drop is still larger than when $L_S/2$ is varied. Thus it may be concluded that for both welded and loose saddles, a dominant factor in the determination of the collapse load is the distance of the saddle to the "head" of the vessel.

4 PARAMETER SURVEY

A recap on the work done so far indicates that, in addition to the basic R/t ratio, the main factors influencing the collapse of horizontal vessels supported on twin saddle supports are:

(a) the fixture of the saddle and vessel, i.e. welded or loose
(b) saddle embracing angle (2α)
(c) saddle width (b_1)
(d) total length of the vessel (L)
(e) distance of the saddle centre profile from the vessel "head" (A)

In order to set the boundaries to a parameter survey to determine the collapse load for a range of vessels, information was used from a survey conducted some years ago by Tooth (7) of actual vessels, built by major vessel fabricators in the U.K. and the U.S.A.

Based on this survey, vessels of A/R ratio equal to 0.5, 1.0, 2.0 and 6.0 and values of $R\alpha/b_1$ (where α is in radians) of 2.0, 3.5, 5.0, 7.5 and 10.0 were examined. This latter grouping is the ratio of half the circumferential saddle length ($R\alpha$) to the width of saddle (b_1) and is similar to the parameter used for stress plots for local loads given in Annex G of the British Standard PD 5500 (1). Various vessel radii of 130mm, 500mm, 1000mm and 4000mm were used. The saddle location was restricted to the quarter point on the vessel but with the vessel's total length varying from *2R, 4R, 8R* and *24R* (representing *A/R* of 0.5, 1.0, 2.0 and 6.0). The saddle embracing angle was restricted to between 120˚ and 150˚ as this corresponds to the extremes of the recommended angles suggested by the Standard (1). The saddle width, saddle embracing angle and the vessel's radius were varied such that the ratio $R\alpha/b_1$ varies from 2, 3.5, 5.0, 7.5 and 10.0. The thickness of the vessels was such that the *R/t* ratio does not exceed 300 to ensure the cases correspond to plastic collapse. The material property of the shell is assumed to be elastic-perfectly plastic with a yield strength of 300N/mm^2. A total of 105 vessels with welded saddles and 113 vessels with loose saddles were analysed to determine the various collapse loads.

The resulting collapse loads were normalised (by dividing by $\sigma_y t^2$) and plotted against $\frac{b_1}{R}\sqrt{\frac{R}{t}}$. This parameter has the merit of combining two variables at the expense of some minor scatter. The results are given in Figs 6(a)-(d) for the welded saddle cases for *A/R* of 0.5, 1.0, 2.0 and 6.0, respectively. The loose saddle results are given in Figs 7(a)-(d). For the case where *A/R* is 0.5, only three values of $R\alpha/b_1$ are used (5.0, 7.5 and 10.0) as the vessel's total length is small. A best-fit line has been shown through all the results for each value of $R\alpha/b_1$. The details of all the geometric cases considered together with the calculated collapse loads are given in the Appendix, Table A1.

Analysis of the welded and loose saddle graphs show that as the vessel becomes longer (larger *A/R*) the collapse load reduces. Increasing the saddle angle, α, (with other parameters constant) results in an increase in collapse load, i.e., $R\alpha/b_1$ increases resulting in a steeper curve. Increasing the ratio $R\alpha/b_1$ seems to imply that by reducing the saddle width, b_1, the collapse load would increase; however, the ratio $\frac{b_1}{R}\sqrt{\frac{R}{t}}$ also reduces. In fact, when the saddle width is reduced the collapse load is also reduced as described earlier. The areas

around the origins represent vessels which have a very low *R/t* ratio and are too thick to be relevant for plastic collapse.

The welded saddle cases have higher collapse loads than the loose saddles. The differences tend to be larger for smaller *R/t* ratios and also as the $R\alpha/b_1$ ratio increases. The survey also shows that as *A/R* is increased (a longer vessel), the differences in collapse load between welded and unwelded cases are smaller. When *A/R*=6.0, the collapse results for both welded and loose saddles are almost identical and even when *A/R*=2.0 the results are very similar. It can be concluded that there is little difference in collapse load when long vessels are employed (*A/R*>6.0). The difference between welded and unwelded reduce with lower $R\alpha/b_1$ (see $R\alpha/b_1$=2.0 for *A/R*=1.0, 2.0 and 6.0), i.e. when saddles are wide and/or saddle angles are small.

5 DESIGN CONSIDERATIONS

From the point of view of application in design situations, it may be useful to have the parametric results in a more directly useable form. Accordingly the best fit curves (8) for the data in Figure 6 and 7, have been characterised in terms of a simple power law of the form,

$$\frac{P}{\sigma_y t^2} = K_1 \left(\frac{R\alpha}{b_1} \right)^n$$

Values of K_1 and n are given in Tables 4 and 5 for the welded and loose saddle cases respectively. Regression coefficient values, R^2, are also included. The 'R^2' is an indicator (not to be confused with *R*, the radius of the vessel) which may range from zero to one and is a measure of how closely the estimated values for the trendline correspond to the actual data. A trendline is most reliable when the R^2 value is at or near 1. Mathematically it is defined as

$$R = 1 - \frac{SSE}{SST}$$

where

$$SSE = \sum (Y_j - \ddot{Y}_j)^2$$

and

$$SST = \left(\sum Y_j^2 \right) - \frac{\left(\sum Y_j \right)^2}{p}$$

where Y_j is the "actual" FE value, $\ddot{Y}_j$ is the curve fit equation result and p is the number of points in the sample. For power law trendlines, Excel uses a transformed regression model. In fact, the error values are remarkably good so that the simple power law equations may be used directly to give estimates of the collapse load. The values of the constants have been given to four decimal places; little is lost if these are rounded to two decimal places.

It is in fact possible to further condense the parametric collapse load results by increasing the combination of geometric parameters, albeit this results in some additional scatter. The results are shown in Figures 8 and 9 for the welded and loose saddle cases against the grouped parameter $\frac{b_1}{\sqrt{Rt}} \left(\frac{R\alpha}{b_1} \right)$. This has the merit of allowing all the results to be shown neatly on one graph. Again these may be fitted with a simple power law of the form,

$$\frac{P}{\sigma_y t^2} = K_2 \left[\frac{b_1}{\sqrt{Rt}} \left(\frac{R\alpha}{b_1} \right)^{0.93} \right]^m$$

for the welded case and

$$\frac{P}{\sigma_y t^2} = K_2 \left[\frac{b_1}{\sqrt{Rt}} \left(\frac{R\alpha}{b_1} \right)^{q} \right]^m$$

for the loose saddle case.

The values of K_2 and m are given in Table 6 for the welded case and in Table 7 for the loose saddle case with the values of q identified in Fig. 9.

6 CONCLUDING COMMENTS

The results in Figures 6 and 7 and the associated reduced data in Tables 4 and 5, Figures 8 and 9 and Table 6 and 7, are useful tools in determining the collapse load of twin saddle supported vessels that may fail by plastic collapse. The validity of these curves is restricted to vessels supported by saddles with embracing angles of 120° to 150° and to the range of parameters covered. They are only valid for failure by plastic collapse; they are not relevant to situations where elastic buckling or fatigue are likely failure modes.

Although the parametric results are for vessels that are supported by twin saddles at the quarter points, they may also be used for vessels, which are not supported at the quarter points. Some guidance can be obtained from Table 3. A simple approach would be to use the *A/R* ratio for that particular vessel since the distance between the supports does not greatly influence the collapse load. When using this approach one must ensure that the appropriate load is used in the calculation.

A possible design approach is to reduce the collapse load obtained from the design curves by 1.5 to obtain a working load. The total load acting on one saddle (fluid and vessel weight) should be less than this working load. If the total load required exceeds the allowable working load, then the design and the allowable working load may be achieved by altering the vessel/saddle parameters.

7 REFERENCES

1 **British Standard PD5500: 2000**, 'Specification for unfired fusion welded pressure vessel, British Standards Institution'.

2 **Chan, G.C.M., Tooth, A.S. and Spence, J.,** 'An experimental study of the collapse of horizontal saddle supported storage vessels.' *Proc Instn Mech Engrs, Vol. 212, 1999, Part E, pp183-195.*

3 **Tooth, A.S., Chan, G.C.M., Spence, J. and Nash, D.H.**, 'Horizontal saddle supported storage vessels: Theoretical and experimental comparisons of plastic collapse loads', *Pressure Vessel Technology – Theory and Practice, Eds. Banks, W M and Nash, D H, IMechE, May 2003*

4 **ANSYS Finite Element Program**, ANSYS Inc. Houston, PA

5 **Zick, L.P.,** 'Stresses in large horizontal cylindrical pressure vessels on two saddle supports', *The Welding Research Supplement IX, Sept 1951, pp435-444.*

6 **Chan, G.C.M.,** 'A design study of the collapse of saddle supported vessels.' PhD thesis, Dept. of Mechanical Engineering, Univ. of Strathclyde, Glasgow, 1995.

7 **Tooth, A.S.** Unpublished survey 1968.

8 **Excel 97,** Microsoft Corporation Ltd.

ACKNOWLEDGEMENTS

The authors would like to thank the UK Government ORS Award Scheme and the University of Strathclyde for the financial support given to Dr. Chan during the course of his study. Use of the ANSYS software through an educational license from ANSYS Inc is also acknowledged. Special thanks are due to Professor Tooth, the initiator of this research work, who died on 11 April 2001.

APPENDIX Tables A 1. Details of vessels and parametric collapse load results

Table A 1a. Welded saddle *A/R*=0.5

Model	t (mm)	R (mm)	b_1 (mm)	2α	P_{ep} (kN)	$P_{ep}/(\sigma_y t^2)$	$(b_1/R)\sqrt{(R/t)}$
$R\alpha/b_1$ = 5.0							
A11	0.5	130	27.23	120	13.49	179.9	3.377
A12	1.0	130	27.23	120	30.66	102.2	2.388
A13	4.0	130	27.23	120	174.76	36.4	1.194
A14	6.0	1000	209.4	120	1306.6	120.98	2.703
A15	13.5	1000	261.8	150	4920.7	90.0	2.253
A16	17.13	1000	261.8	150	6734.4	76.5	2.0
A17	35.0	1000	261.8	150	15420.0	41.95	1.4
$R\alpha/b_1$ = 7.5							
F11	7.0	1000	139.6	120	1641.5	111.7	1.67
F12	17.13	1000	174.53	150	6607.5	75.1	1.33
F13	19.15	1000	139.6	120	5526.9	50.23	1.0
F14	14.3	4000	558.5	120	11438.1	186.4	2.33
F15	30.5	4000	698.1	150	39793.4	142.6	2.0
$R\alpha/b_1$ = 10.0							
B11	7.0	1000	104.6	120	1407.2	95.7	1.25
B12	17.13	1000	130.9	150	6309.9	71.67	1.0
B13	19.5	1000	104.7	120	5494.6	48.16	0.75
B14	14.3	4000	418.8	120	11257.3	183.5	1.75
B15	30.5	4000	523.6	150	35814.2	128.3	1.50

Table A 1b. Welded saddle *A/R*=1.0

Model	t (mm)	R (mm)	b_1 (mm)	2α	P_{ep} (kN)	$P_{ep}/(\sigma_y t^2)$	$(b_1/R)\sqrt{(R/t)}$
$R\alpha/b_1$ = 2.0							
D21	2.14	500	261.8	120	230.4	167.7	8.0
D22	23.8	500	327.2	150	6184.1	36.39	3.0
D23	11.0	1000	523.6	120	2904.0	80.0	5.0
D24	11.9	1000	654.5	150	4503.2	106.0	6.0
D25	68.5	1000	523.6	120	30780.0	21.86	2.0
D26	35.0	4000	2618.0	150	48747.2	132.9	7.0
D27	68.5	4000	2094.4	120	84848.3	60.27	4.0
$R\alpha/b_1$ = 3.5							
C21	3.45	500	187.0	150	538.6	150.5	4.5
C22	4.37	500	187.0	150	673.2	117.5	4.0
C23	19.9	500	149.6	120	3590.4	30.22	1.5
C24	3.25	1000	299.2	120	574.5	181.3	5.248
C25	35.0	1000	374.0	150	15633.2	42.54	2.0
C26	40.0	4000	1196.8	120	39770.6	83.77	3.0
$R\alpha/b_1$ = 5.0							
A21	0.5	130	27.23	120	11.65	155.3	3.377
A22	1.0	130	27.23	120	27.59	91.98	2.388
A23	2.0	130	27.23	120	70.52	58.76	1.688
A24	4.0	130	27.23	120	177.6	37.0	1.194
A25	6.0	1000	209.4	120	1268.0	117.4	2.703
A26	13.5	1000	261.8	150	4725.5	86.4	2.253
A27	35.0	1000	261.8	150	15696.4	42.7	1.4
$R\alpha/b_1$ = 7.5							
F21	7.0	1000	139.6	120	1429.7	97.26	1.668
F22	17.13	1000	174.5	150	6300.5	71.53	1.33
F23	19.5	1000	139.6	120	5213.2	45.7	1.0
F24	14.3	4000	558.5	120	10365.8	169.0	2.335
F25	30.5	4000	698.1	150	37405.8	134.03	2.0
$R\alpha/b_1$ = 10.0							
B21	7.0	1000	104.7	120	1440.6	98.0	1.251
B22	17.13	1000	130.9	150	6217.7	70.63	1.0
B23	19.5	1000	104.7	120	5360.6	47.0	0.75
B24	14.3	4000	418.8	120	9814.1	160.0	1.751
B25	30.5	4000	523.6	150	36610.0	131.2	1.5

Table A 1c. Welded saddle *A/R*=2.0

Model	t (mm)	R (mm)	b_1 (mm)	2α	P_{ep} (kN)	$P_{ep}/(\sigma_y t^2)$	$(b_1/R)\sqrt{(R/t)}$
$R\alpha/b_1$ = 2.0							
D31	2.14	500	261.8	120	150.8	109.8	8.0
D32	8.6	500	327.2	150	1397.4	62.98	5.0
D33	23.8	500	327.2	150	5595.1	32.92	3.0
D34	11.9	1000	654.5	150	3332.7	78.44	6.0
D35	68.5	1000	523.6	120	28435.0	20.2	2.0
D36	35.0	4000	2618.0	150	37008.0	100.9	7.0
D37	68.5	4000	2094.4	120	61659.1	43.8	4.0
$R\alpha/b_1$ = 3.5							
C31	3.45	500	187.0	150	377.6	105.5	4.5
C32	4.37	500	187.0	150	525.9	91.79	4.0
C33	20.0	500	149.6	120	3261.6	28.18	1.5
C34	4.0	1000	299.2	120	571.2	119.0	4.731
C35	35.0	1000	374.0	150	13501.4	36.74	2.0
C36	40.0	4000	1196.8	120	28824.0	60.05	3.0
$R\alpha/b_1$ = 5.0							
A31	0.5	130	27.23	120	7.91	105.5	3.377
A32	1.0	130	27.23	120	19.00	63.3	2.388
A33	4.0	130	27.23	120	132.1	27.51	1.194
A34	6.0	1000	209.4	120	827.5	76.62	2.703
A35	11.0	1000	209.4	120	2004.1	55.21	2.0
A36	13.5	1000	261.8	150	3481.9	62.5	2.253
A37	35.0	1000	261.8	150	12435.5	33.83	1.4
$R\alpha/b_1$ = 7.5							
F31	7.0	1000	139.6	120	982.9	66.86	1.668
F32	17.13	1000	174.5	150	4642.5	52.74	1.33
F33	19.5	1000	139.6	120	3842.9	33.68	1.0
F34	16.0	4000	558.5	120	8233.0	107.2	2.207
F35	30.5	4000	698.1	150	25783.7	92.39	2.0
$R\alpha/b_1$ = 10.0							
B31	7.0	1000	104.7	120	964.0	65.58	1.251
B32	17.13	1000	130.9	150	4568.8	51.9	1.0
B33	19.5	1000	104.7	120	3422.2	30.0	0.75
B34	16.0	4000	418.8	120	8388.1	109.2	1.655
B35	30.5	4000	523.6	150	25865.8	92.68	1.5

Table A 1d. Welded saddle *A/R*=6.0

Model	t (mm)	R (mm)	b_1 (mm)	2α	P_{ep} (kN)	$P_{ep}/(\sigma_y t^2)$	$(b_1/R)\sqrt{(R/t)}$
$R\alpha/b_1$ = 2.0							
D41	23.8	500	327.2	150	2679.8	15.77	3.0
D42	11.0	1000	523.6	120	1139.3	31.58	5.0
D43	12.0	1000	654.5	150	1802.9	42.44	6.0
D44	68.5	1000	523.6	120	15414.8	10.95	2.0
D45	35.0	4000	2618.0	150	17907.1	48.81	7.0
D46	68.5	4000	2094.5	120	38872.0	27.6	4.0
$R\alpha/b_1$ = 3.5							
C41	3.45	500	187.0	150	199.0	54.14	4.5
C42	4.37	500	187.0	150	258.0	45.04	4.0
C43	20.0	500	149.6	120	2065.6	17.39	1.5
C44	35.0	1000	374.0	120	7816.6	21.27	2.0
C45	40.0	4000	1196.8	120	16085.0	33.88	3.0
$R\alpha/b_1$ = 5.0							
A41	1.0	130	27.23	120	12.14	40.48	2.388
A42	2.0	130	27.23	120	36.58	30.48	1.688
A43	4.0	130	27.23	120	96.0	20.0	1.194
A44	7.61	1000	261.8	150	870.5	50.03	3.0
A45	13.5	1000	261.8	150	2089.2	38.21	2.25
A46	17.17	1000	261.8	150	3084.0	34.85	2.0
A47	35.0	1000	261.8	150	8209.9	22.34	1.4
$R\alpha/b_1$ = 7.5							
F41	7.0	1000	139.6	120	536.1	36.47	1.668
F42	17.13	1000	174.5	150	2918.1	33.14	1.33
F43	19.5	1000	139.6	120	2904.5	25.46	1.0
F44	25.0	1000	139.6	120	4245.1	22.64	0.883
F45	30.5	4000	698.1	150	13441.7	48.16	2.0
$R\alpha/b_1$ = 10.0							
B41	7.0	1000	104.7	120	552.3	37.57	1.251
B42	17.13	1000	130.9	150	2984.5	33.9	1.0
B43	19.5	1000	104.7	120	2931.6	25.7	0.75
B44	20.0	1000	130.9	150	3570.0	29.75	0.925
B45	30.5	4000	523.6	150	13795.1	49.43	1.5

Table A 1e. Loose saddle *A/R*=0.5

Model	t (mm)	R (mm)	b_1 (mm)	2α	P_{ep} (kN)	$P_{ep}/(\sigma_y t^2)$	$(b_1/R)\sqrt{(R/t)}$
$R\alpha/b_1$ = 5.0							
LA11	0.5	130	27.23	120	9.65	128.7	3.377
LA12	1.0	130	27.23	120	23.3	77.67	2.388
LA13	4.0	130	27.23	120	145.5	30.3	1.194
LA14	6.0	1000	209.4	120	965.6	89.41	2.703
LA15	13.5	1000	261.8	150	3925.5	71.8	2.253
LA16	17.13	1000	261.8	150	5281.9	60.0	2.0
LA17	35.0	1000	261.8	150	12849.8	34.96	1.4
$R\alpha/b_1$ = 7.5							
LF11	7.0	1000	139.6	120	1000.1	68.03	1.67
LF12	17.13	1000	174.53	150	4476.7	50.85	1.33
LF13	19.15	1000	139.6	120	3946.7	34.60	1.0
LF14	16.0	4000	558.5	120	7923.4	103.2	2.33
LF15	30.5	4000	698.1	150	25516.1	91.43	2.0
$R\alpha/b_1$ = 10.0							
LB11	5.0	1000	130.9	150	825.0	110.0	1.851
LB12	7.0	1000	104.7	120	894.5	60.83	1.251
LB13	17.13	1000	130.9	150	4419.3	49.22	1.0
LB14	19.5	1000	104.7	120	3567.8	31.28	0.75
LB15	16.0	4000	418.8	120	6798.3	88.52	1.655
LB16	30.5	4000	523.6	150	21779.4	78.04	1.50

Table A 1f. Loose saddle *A/R*=1.0

Model	t (mm)	R (mm)	b_1 (mm)	2α	P_{ep} (kN)	$P_{ep}/(\sigma_y t^2)$	$(b_1/R)\sqrt{(R/t)}$
$R\alpha/b_1$ = 2.0							
LD21	2.14	500	261.8	120	193.7	141.0	8.0
LD22	23.8	500	327.2	150	6180.0	36.37	3.0
LD23	11.0	1000	523.6	120	2881.6	79.88	5.0
LD24	11.9	1000	654.5	150	4352.4	102.4	6.0
LD25	68.5	1000	523.6	120	32830.1	23.32	2.0
LD26	35.0	4000	2618.0	150	47183.3	128.6	7.0
LD27	68.5	4000	2094.4	120	83105.8	59.04	4.0
$R\alpha/b_1$ = 3.5							
LC21	3.45	500	187.0	150	465.4	130.02	4.5
LC22	4.37	500	187.0	150	673.2	117.5	4.0
LC23	19.9	500	149.6	120	3270.7	27.53	1.5
LC24	4.0	1000	299.2	120	681.6	142.0	4.731
LC25	35.0	1000	374.0	150	14948.9	40.68	2.0
LC26	40.0	4000	1196.8	120	35042.3	73.81	3.0
$R\alpha/b_1$ = 5.0							
LA21	0.5	130	27.23	120	7.97	106.27	3.377
LA22	1.0	130	27.23	120	21.16	70.52	2.388
LA23	4.0	130	27.23	120	134.9	28.11	1.194
LA24	3.58	1000	209.4	120	435.5	113.3	3.5
LA25	6.0	1000	209.4	120	904.6	83.76	2.703
LA26	13.5	1000	261.8	150	3730.6	68.23	2.253
LA27	19.0	1000	261.8	150	5921.8	54.76	1.9
LA28	35.0	1000	261.8	150	12276.3	33.4	1.4
$R\alpha/b_1$ = 7.5							
LF21	4.87	1000	174.5	150	798.7	112.1	2.5
LF22	7.0	1000	139.6	120	869.3	59.14	1.67
LF23	17.13	1000	174.5	150	4475.4	50.84	1.33
LF24	19.5	1000	139.6	120	3920.5	34.37	1.0
LF25	17.0	4000	558.5	120	7863.7	90.7	2.14
LF26	30.5	4000	698.1	150	22814.9	81.75	2.0
$R\alpha/b_1$ = 10.0							
LB21	7.0	1000	104.7	120	804.1	54.7	1.251
LB22	17.13	1000	130.9	150	3772.2	42.85	1.0
LB23	19.5	1000	104.7	120	3350.4	29.37	0.75
LB24	16.0	4000	418.8	120	5896.7	76.78	1.655
LB25	19.0	4000	523.6	150	10883.5	100.6	1.9
LB26	30.5	4000	523.6	150	19718.1	70.65	1.5

Table A 1g. Loose saddle *A/R*=2.0

Model	t (mm)	R (mm)	b_1 (mm)	2α	P_{ep} (kN)	$P_{ep}/(\sigma_y t^2)$	$(b_1/R)\sqrt{(R/t)}$
$R\alpha/b_1$ = 2.0							
LD31	2.14	500	261.8	120	154.6	112.5	8.0
LD32	8.6	500	327.2	150	1353.8	61.51	5.0
LD33	23.8	500	327.2	150	5801.2	34.14	3.0
LD34	11.9	1000	654.5	150	3100.2	72.97	6.0
LD35	68.5	1000	523.6	120	27731.2	19.7	2.0
LD36	35.0	4000	2618.0	150	33824.6	92.2	7.0
LD37	68.5	4000	2094.4	120	61010.4	43.34	4.0
$R\alpha/b_1$ = 3.5							
LC31	3.45	500	187.0	150	361.8	101.1	4.5
LC32	4.37	500	187.0	150	509.7	88.97	4.0
LC33	20.0	500	149.6	120	3051.8	25.69	1.5
LC34	4.0	1000	299.2	120	500.6	104.3	4.731
LC35	35.0	1000	374.0	150	11943.7	32.5	2.0
LC36	40.0	4000	1196.8	120	27086.4	56.43	3.0
$R\alpha/b_1$ = 5.0							
LA31	0.5	130	27.23	120	6.84	91.22	3.377
LA32	1.0	130	27.23	120	19.04	63.47	2.388
LA33	4.0	130	27.23	120	130.6	27.21	1.194
LA34	5.0	1000	261.8	150	806.2	107.5	3.69
LA35	6.0	1000	209.4	120	780.6	72.28	2.703
LA36	11.0	1000	209.4	120	1760.8	48.84	2.0
LA37	13.5	1000	261.8	150	3382.4	61.86	2.25
LA38	35.0	1000	261.8	150	11861.5	32.28	1.4
$R\alpha/b_1$ = 7.5							
LF31	4.0	1000	174.5	150	530.1	110.4	2.76
LF32	7.0	1000	139.6	120	840.0	57.14	1.67
LF33	17.13	1000	174.5	150	4017.1	45.63	1.33
LF34	19.5	1000	139.6	120	3574.8	31.34	1.0
LF35	16.0	4000	558.5	120	6255.2	81.45	2.207
LF36	30.5	4000	698.1	150	21223.1	76.05	2.0
$R\alpha/b_1$ = 10.0							
LB31	4.0	1000	130.9	150	456.0	95.0	2.07
LB32	7.0	1000	104.7	150	702.9	47.82	1.251
LB33	17.3	1000	130.9	150	3450.0	38.42	1.0
LB34	19.5	1000	104.7	120	3224.8	28.27	0.75
LB35	16.0	4000	418.8	120	5377.5	70.02	1.655
LB36	30.5	4000	523.6	150	17680.0	63.35	1.50

Table A 1h. Loose saddle *A/R*=6.0

Model	t (mm)	R (mm)	b_1 (mm)	2α	P_{ep} (kN)	$P_{ep}/(\sigma_y t^2)$	$(b_1/R)\sqrt{(R/t)}$
$R\alpha/b_1$ = 2.0							
LD41	23.8	500	327.2	150	2503.1	14.73	3.0
LD42	11.0	1000	523.6	120	1125.3	31.19	5.0
LD43	12.0	1000	654.5	150	1837.3	43.25	6.0
LD44	68.5	1000	523.6	120	14355.8	10.19	2.0
LD45	35.0	4000	2618.0	150	17364.4	47.25	7.0
LD46	68.5	4000	2094.5	120	40212.5	28.57	4.0
$R\alpha/b_1$ = 3.5							
LC41	3.45	500	187.0	150	183.0	51.14	4.5
LC42	4.37	500	187.0	150	265.3	46.31	4.0
LC43	11.2	500	187.0	150	1057.7	28.15	2.5
LC44	19.9	500	149.6	120	1952.0	16.43	1.5
LC45	35.0	1000	374.0	120	7106.0	19.34	2.0
LC46	40.0	4000	1196.8	120	15794.7	33.27	3.0
$R\alpha/b_1$ = 5.0							
LA41	1.0	130	27.23	120	11.65	38.84	2.388
LA42	2.0	130	27.23	120	33.69	28.08	1.688
LA43	4.0	130	27.23	120	91.41	19.04	1.194
LA44	7.61	1000	261.8	150	828.7	47.66	3.0
LA45	13.5	1000	261.8	150	2030.2	37.13	2.253
LA46	17.17	1000	261.8	150	2878.3	32.52	2.0
LA47	35.0	1000	261.8	150	7794.3	21.21	1.4
$R\alpha/b_1$ = 7.5							
LF41	7.0	1000	139.6	120	548.5	37.31	1.67
LF42	17.13	1000	174.5	150	2875.0	32.66	1.33
LF43	19.5	1000	139.6	120	2748.1	24.1	1.0
LF44	25.0	1000	139.6	120	3881.1	20.7	0.883
LF45	30.5	4000	698.1	150	13204.4	47.31	2.0
$R\alpha/b_1$ = 10.0							
LB41	7.0	1000	104.7	120	543.0	36.94	1.251
LB42	17.13	1000	130.9	150	2821.4	32.05	1.0
LB43	19.5	1000	104.7	120	2680.3	23.5	0.75
LB44	20.0	1000	130.9	150	3300.0	27.5	0.925
LB45	30.5	4000	523.6	150	12816.7	45.92	1.5

Table 1. Variation of collapse load with the saddle width (welded saddle).

Saddle Width b_1 (mm)	Collapse Load P (kN)
b_1 (10)	38.70
2 b_1 (20)	39.07
3 b_1 (30)	40.50
4 b_1 (40)	42.52
5 b_1 (50)	43.31

Table 2. Comparison of collapse loads for experimental and F.E. end supported inverted case models with F.E. "actual" models.

Welded Saddle (*R*=130mm, *L*=555mm, *2α*=120°, b_1=10mm)					
			Collapse load (kN)		
Vessel No.	*t* (mm)	σ_y (N/mm^2)	Experimental	F.E. end supported	F.E. "actual"
1	0.97	160.5	16.61	16.20	10.01
2	1.22	222.2	29.85	28.12	17.77
3	1.57	222.2	44.50	38.70	23.29
4	2.08	214.0	64.52	53.43	35.70
Loose Saddle (*R*=130mm, *L*=555mm, *2α*=120°, b_1=10mm)					
			Collapse load (kn)		
Vessel No.	*t* (mm)	σ_y (N/mm^2)	Experimental	F.E. end supported	F.E. "actual"
5	0.97	160.5	7.55	7.28	7.28
6	1.13	275.0	17.00	14.50	14.33
7	1.55	275.0	24.47	22.48	21.56
8	2.08	214.0	32.73	28.55	28.10

Table 3. Variation of collapse load with the position of the saddle (See text for geometric parameters)

Welded Saddle (Vessel No. 3)			**Loose Saddle (Vessel No. 7)**		
A	$L_S/2$	*P* (kN)	*A*	L_S/2	*P* (kN)
2R	*R*	23.17	*2R*	*R*	20.81
2R	*2R*	23.29	*2R*	*2R*	21.56
2R	*3R*	24.55	*2R*	*3R*	22.44
2R	*4R*	25.00	*2R*	*4R*	22.52
R	*2R*	32.17	*R*	*2R*	23.10
2R	*2R*	23.29	*2R*	*2R*	21.56
3R	*2R*	18.00	*3R*	*2R*	19.95
4R	*2R*	15.30	*4R*	*2R*	18.40

Table 4. Graph curve-fit constants for welded saddle geometries

Welded Case	$R\alpha/b_1$	K_1	n	Error R^2
A/R=0.5	2	72.159	1.5324	0.9880
	3.5	49.541	1.5512	0.9984
	5	26.104	1.5582	0.9959
A/R=1.0	10	71.198	1.4604	0.9994
	7.5	45.598	1.5391	0.9989
	5	27.737	1.4136	0.9964
	3.5	16.301	1.4558	0.9970
	2	7.6067	1.4741	0.9981
A/R=2.0	10	71.257	1.4752	0.9993
	7.5	45.598	1.5391	0.9989
	5	27.737	1.4136	0.9964
	3.5	16.301	1.4558	0.9970
	2	7.6067	1.4741	0.9981
A/R=6.0	2	32.791	0.905	0.9657
	3.5	25.264	0.8655	0.9764
	5	16.77	1.0175	0.9866
	7.5	10.916	1.0386	0.9926
	10	4.5069	1.2345	0.9852

Table 5. Graph curve-fit constants for loose saddle geometries

Loose Case	$R\alpha/b_1$	K_1	n	Error R^2
A/R=0.5	2	22.624	1.4107	0.9966
	3.5	34.802	1.325	0.9955
	5	46.574	1.329	0.993
A/R=1.0	10	8.8437	1.3558	0.9956
	7.5	15.309	1.4278	0.9987
	5	22.566	1.3041	0.995
	3.5	33.852	1.2799	0.9857
	2	42.139	1.2798	0.9945
A/R=2.0	10	8.4071	1.229	0.9955
	7.5	14.317	1.2863	0.9927
	5	21.862	1.2076	0.9954
	3.5	31.453	1.2297	0.997
	2	38.663	1.195	0.9947
A/R=6.0	2	4.0715	1.2906	0.9725
	3.5	10.034	1.0889	0.9866
	5	15.751	1.0323	0.9922
	7.5	23.812	0.9684	0.9896
	10	30.707	0.9562	0.9842

Table 6. Graph curve-fit constants for welded saddle condensed data

A/R	K_2	***m***	**Error R^2**
0.5	2.58	1.56	0.993
1.0	3.00	1.47	0.996
2.0	3.22	1.30	0.983
6.0	3.08	1.08	0.952

Table 7. Graph curve-fit constants for loose saddle condensed data

A/R	K_2	***m***	**Error R^2**
0.5	5.07	1.363	0.994
1.0	4.89	1.340	0.990
2.0	4.25	1.233	0.988
6.0	2.66	1.126	0.959

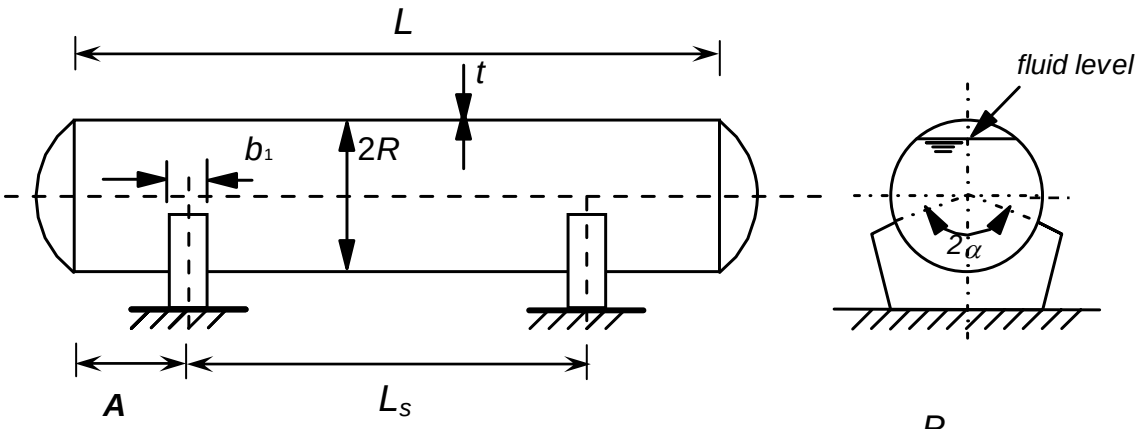

Figure 1a.

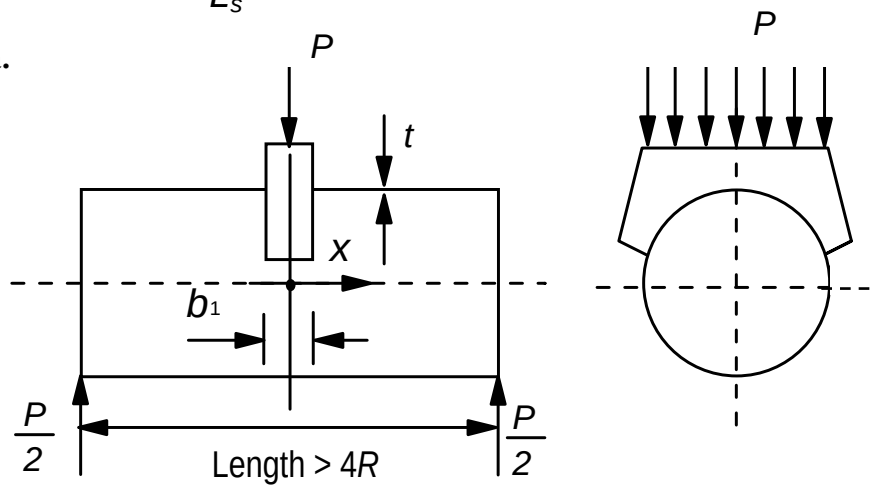

Figure 1b.

Figure 1. Geometric details of saddle supported vessel and simple test arrangement

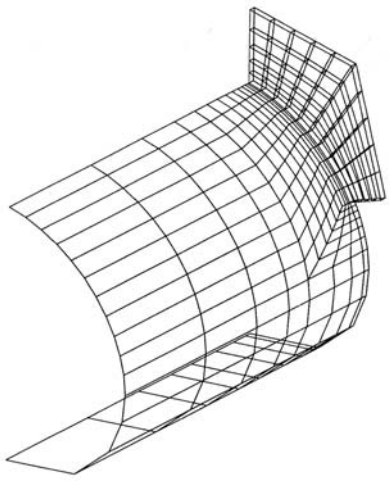

Figure 2. Finite element model of "end supported inverted case" vessel

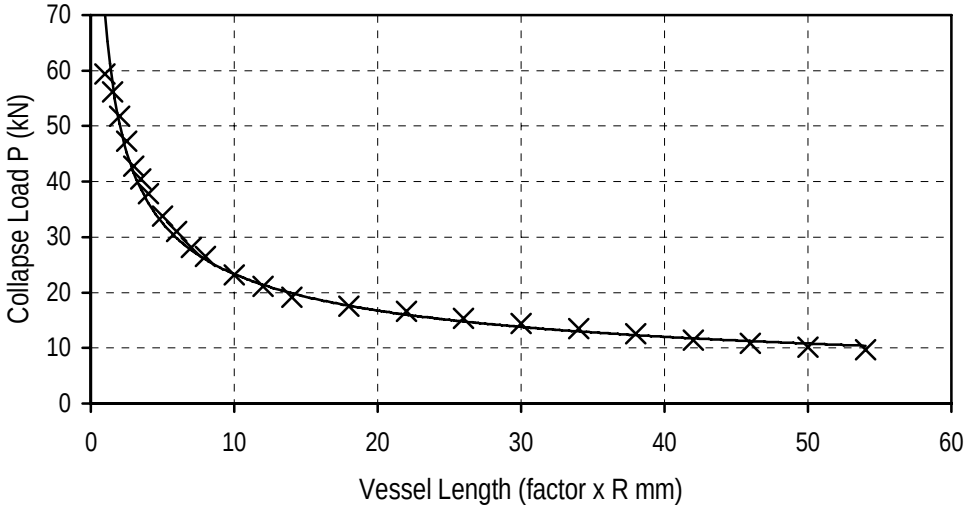

Figure 3. Variation of the collapse load with vessel length (welded case)

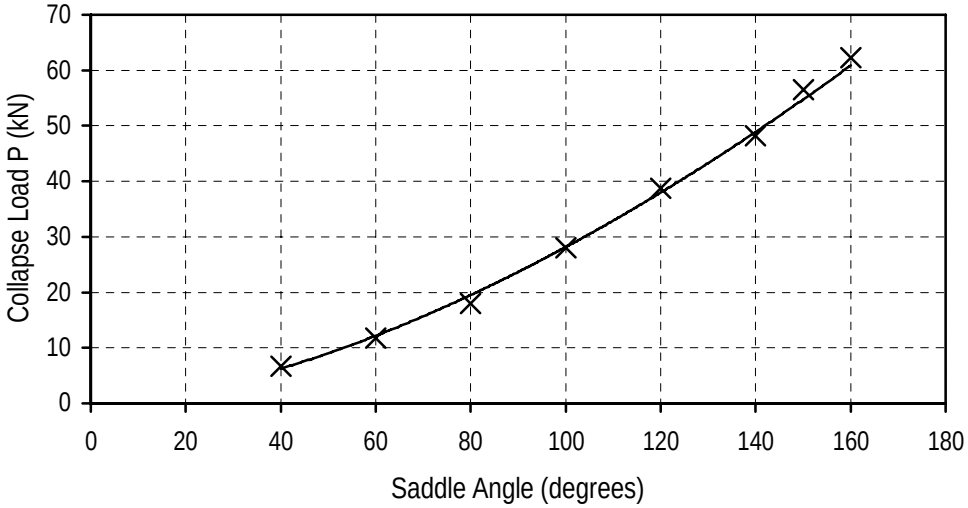

Figure 4. Variation of the collapse load with saddle angle (welded case)

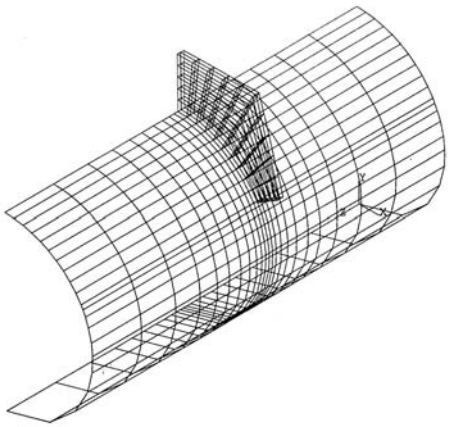

Figure 5. Finite element model of "actual" vessel

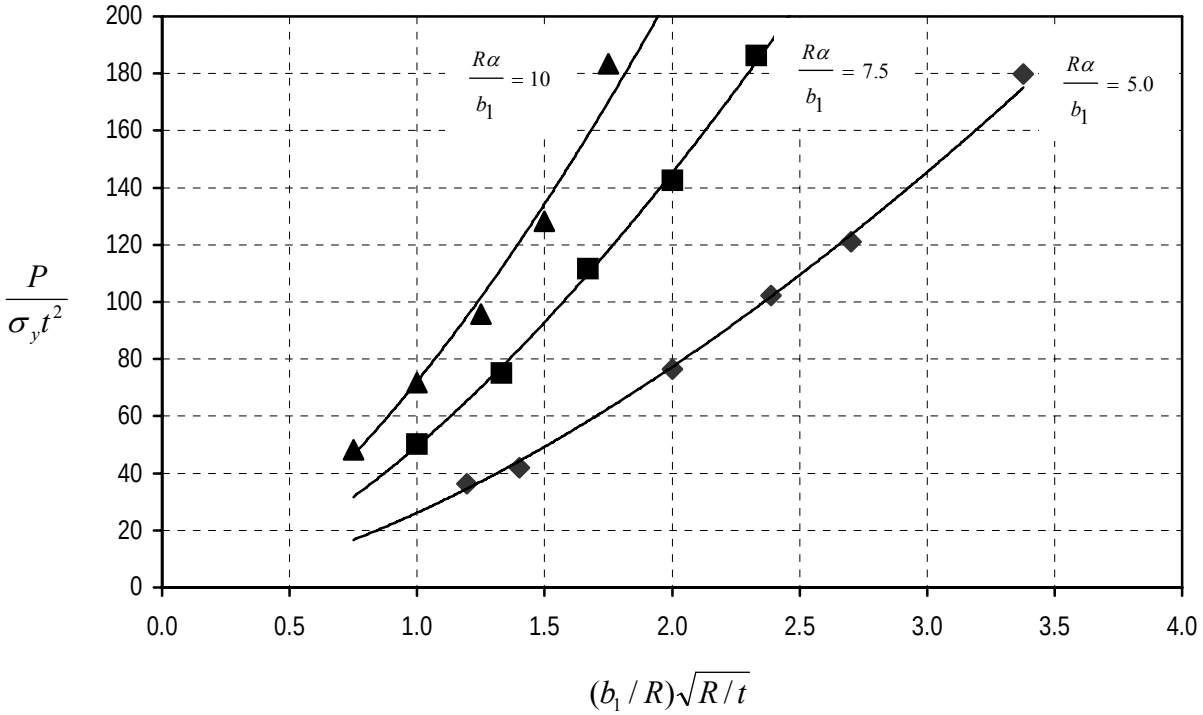

Figure 6a. Collapse curves for welded saddle vessels for *A/R*=0.5

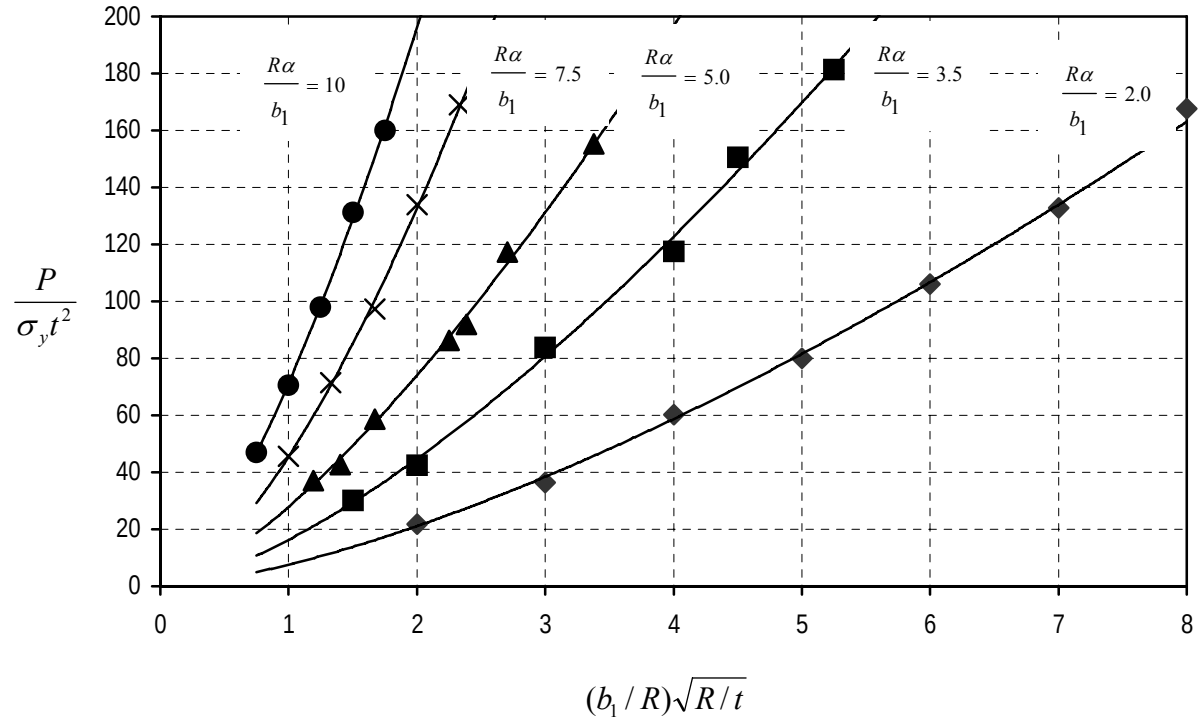

Figure 6b. Collapse curves for welded saddle vessels for *A/R*=1.0

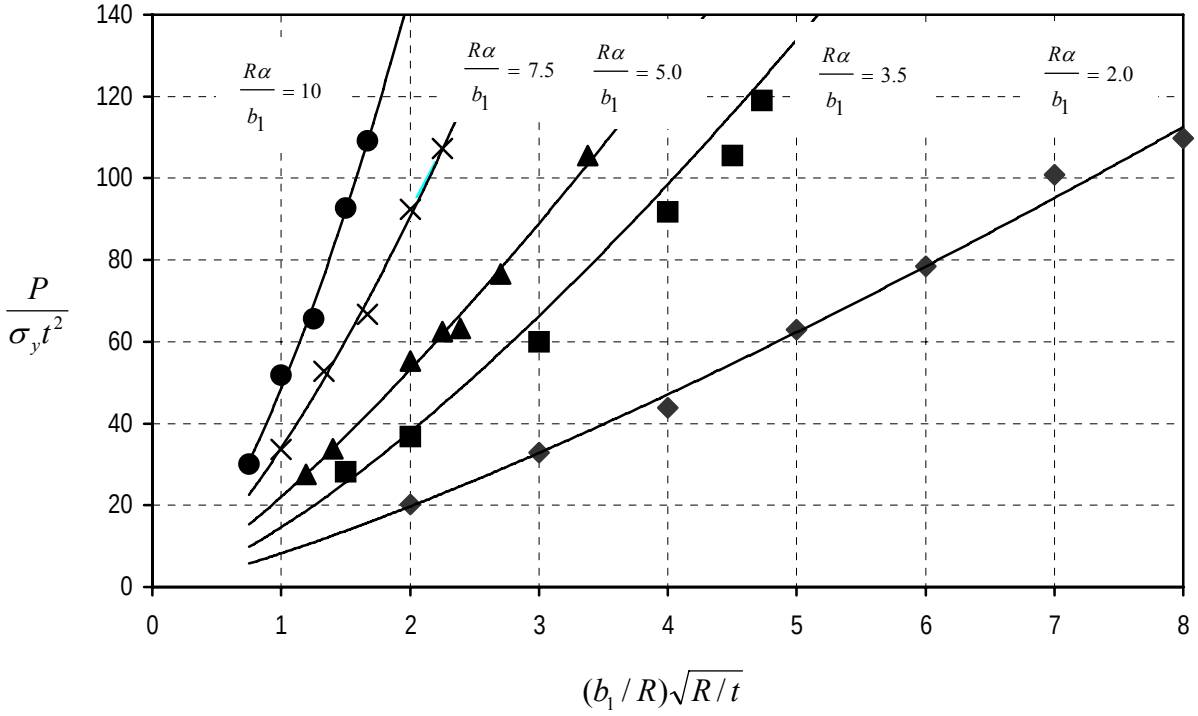

Figure 6c. Collapse curves for welded saddle vessels for *A/R*=2.0

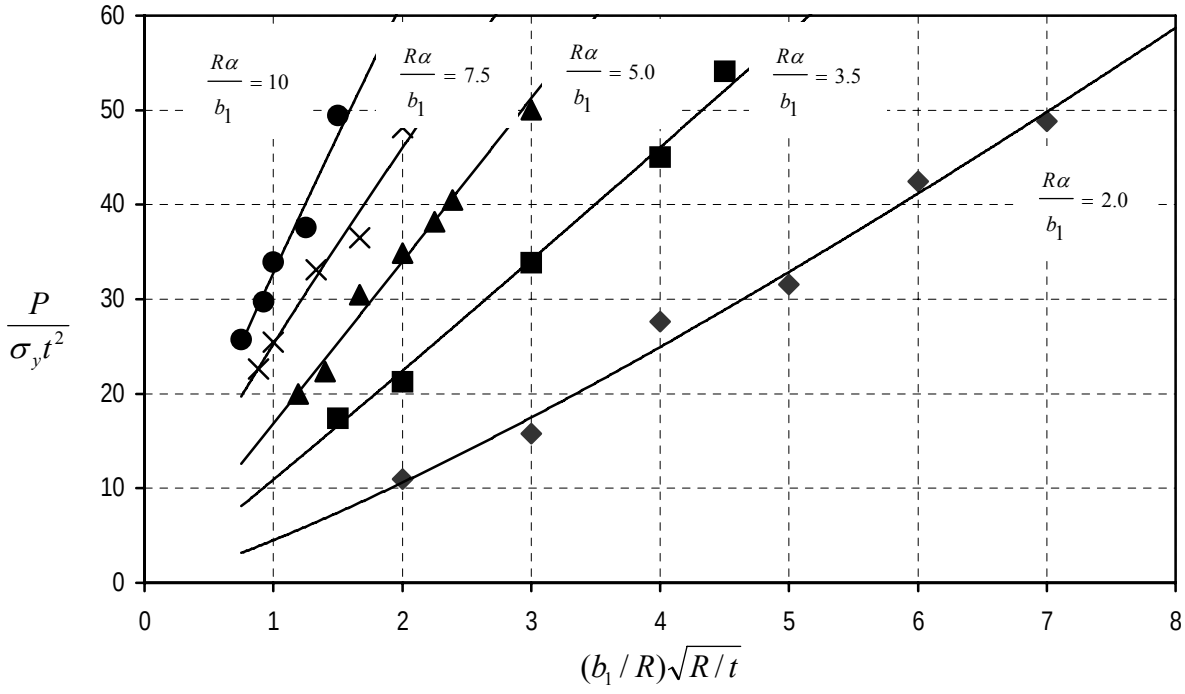

Figure 6d. Collapse curves for welded saddle vessels for *A/R*=6.0

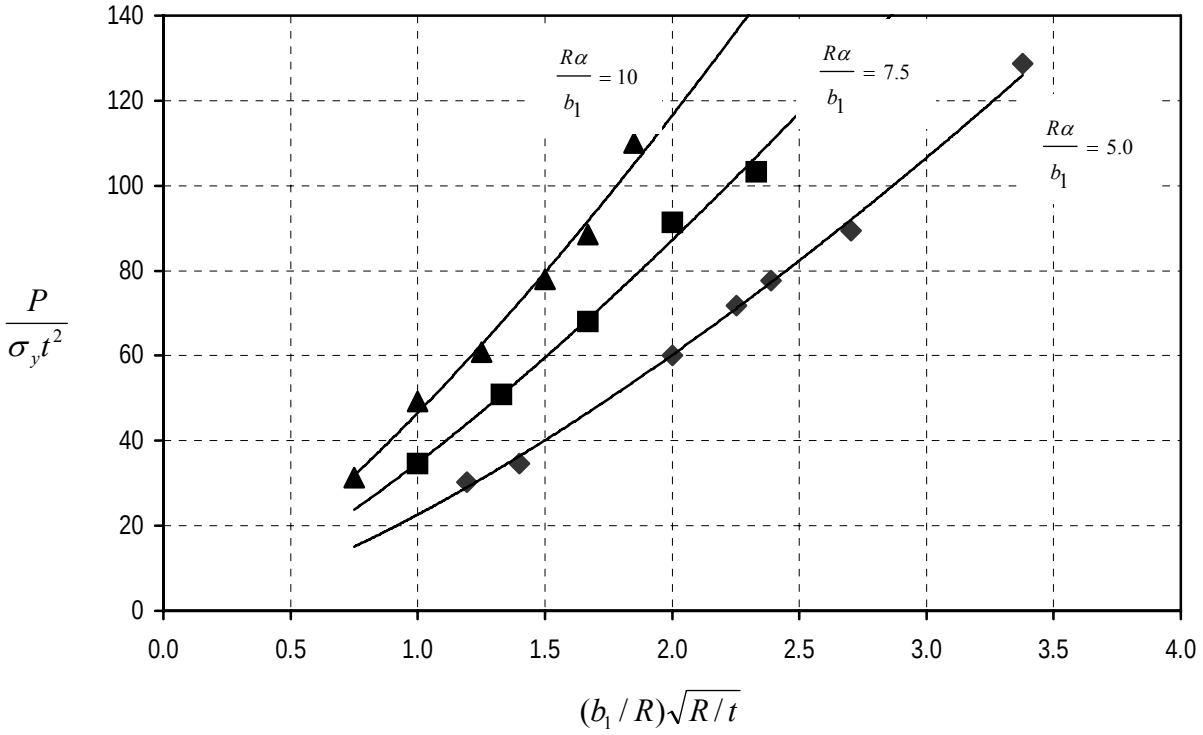

Figure 7a. Collapse curves for loose saddle vessels for *A/R*=0.5

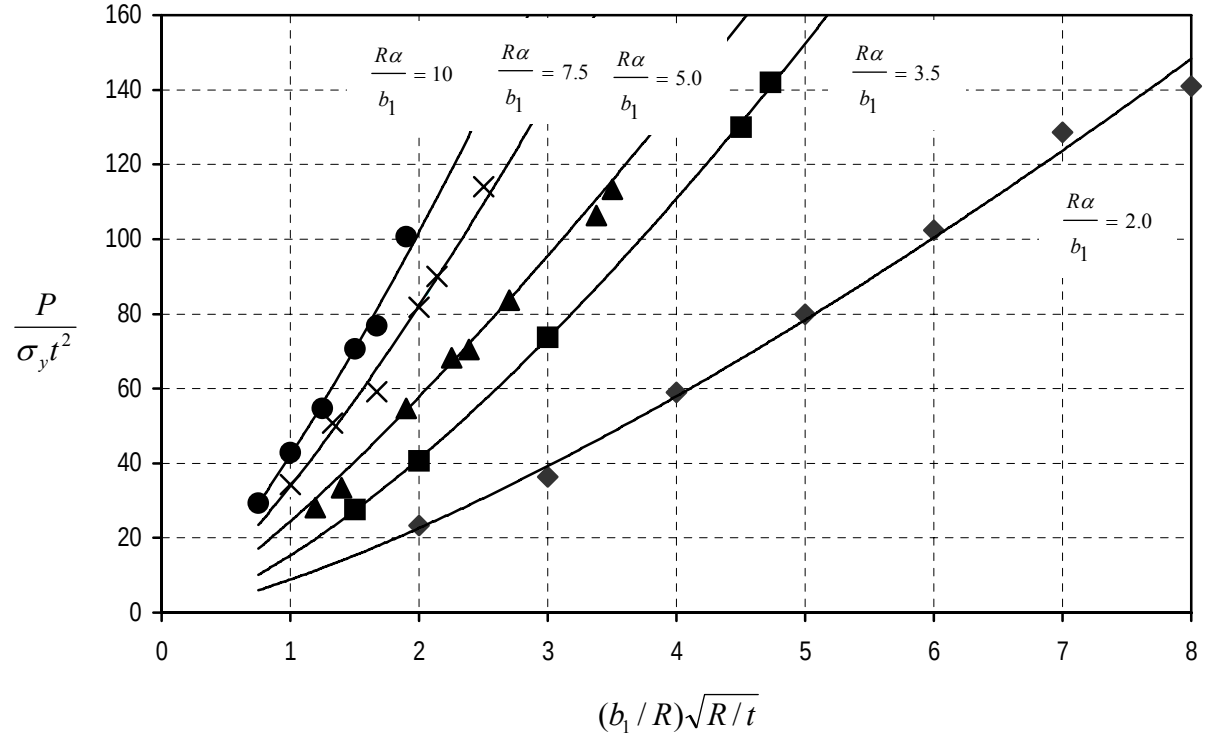

Figure 7b. Collapse curves for loose saddle vessels for *A/R*=1.0

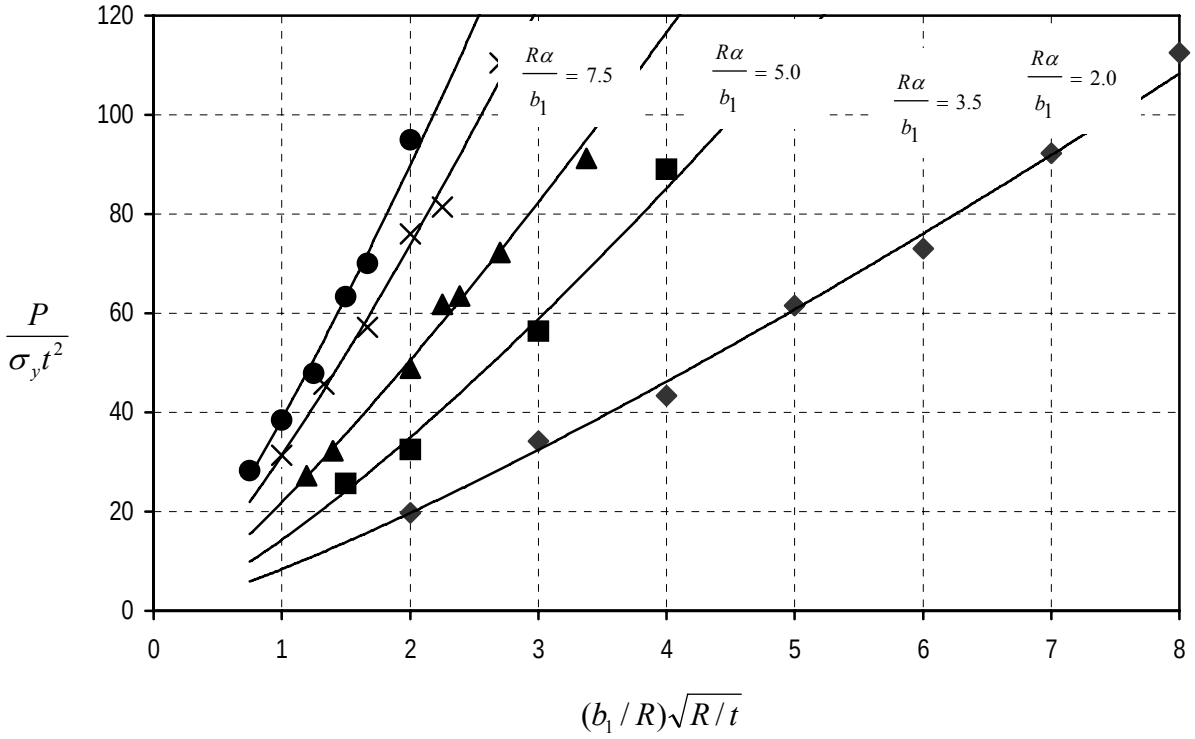

Figure 7c. Collapse curves for loose saddle vessels for *A/R*=2.0

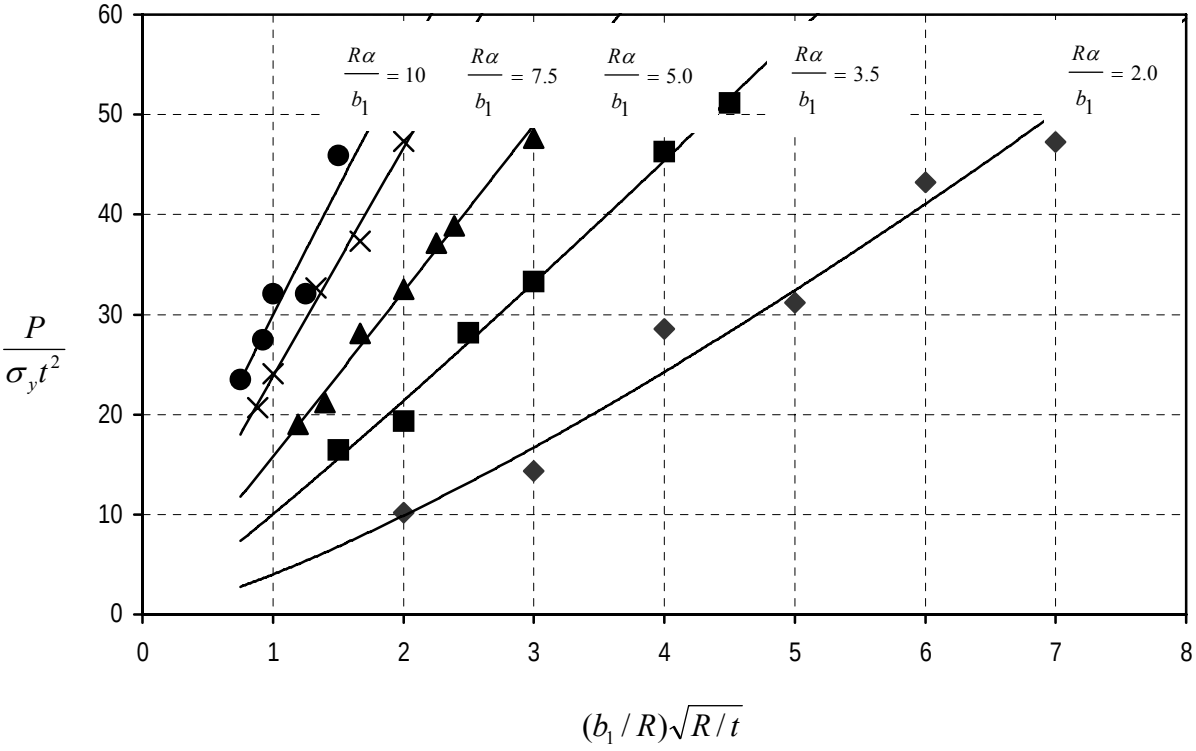

Figure 7d. Collapse curves for loose saddle vessels for *A/R*=6.0

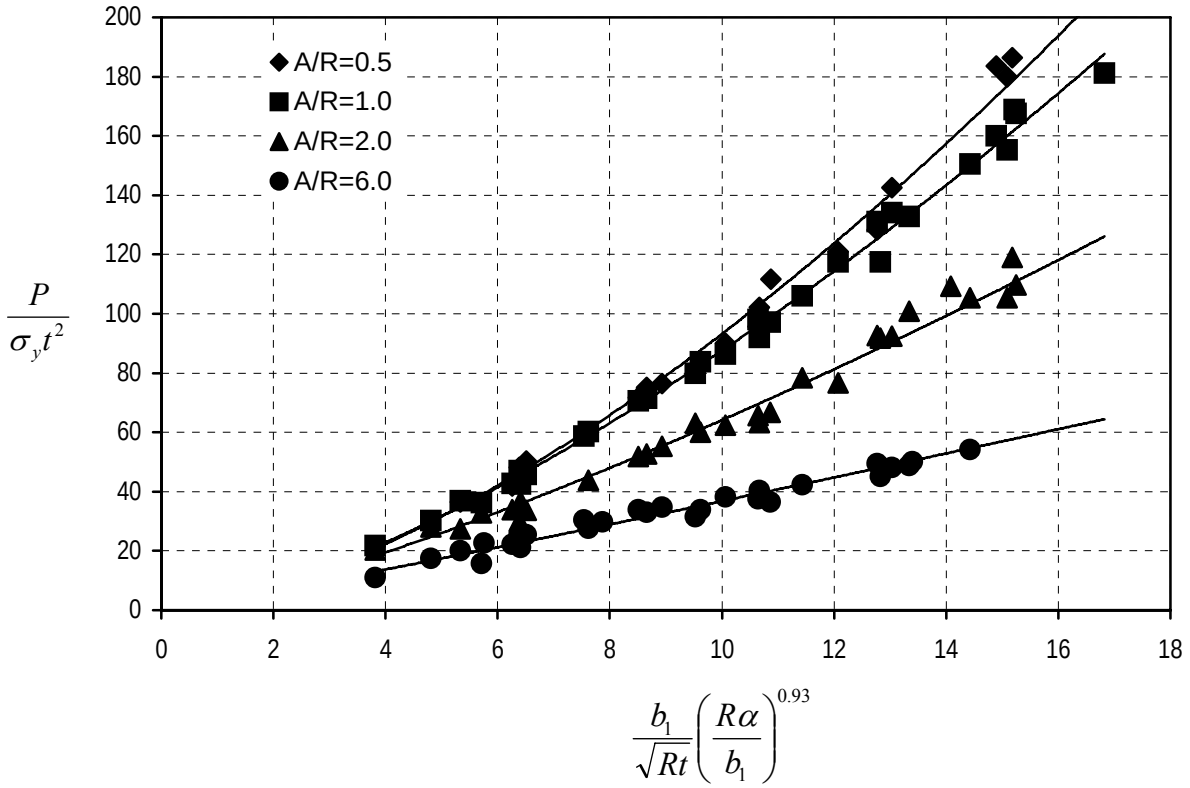

Figure 8. Condensed Plot of Collapse Loads for Welded Saddle Cases

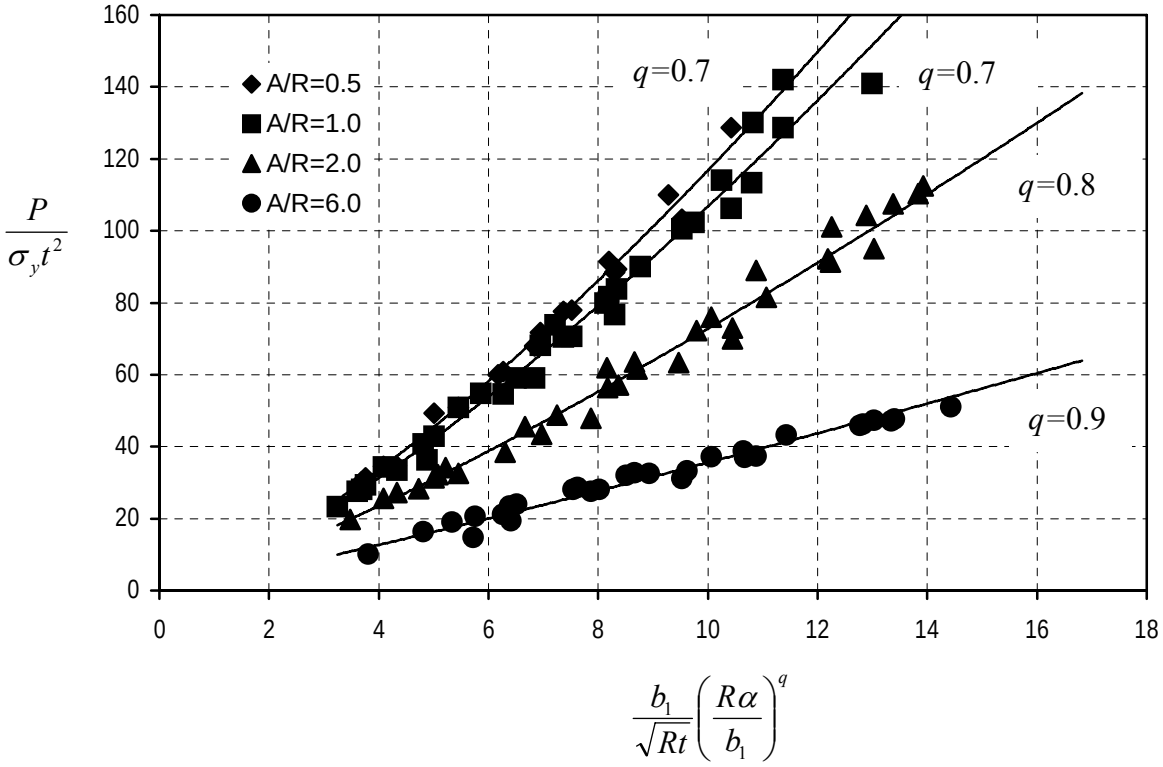

Figure 9. Condensed Plot of Collapse Loads for Loose Saddle Cases